Effect of Cu- and Y-Codoping on Structural and Luminescent Properties of Zirconia Based Nanopowders

N. Korsunska[a], T. Stara[a], L. Khomenkova[a], Yu. Poslishchuk[a],
V. Kladko[a], K. Michailovska[a], M. Kharchenko[b] and O. Gorban[b]

[a] V.Lashkaryov Institute of Semiconductor Physics of NAS of Ukraine,
45 Pr. Nauky, Kyiv 03028, Ukraine
[b] Donetsk Institute for Physics and Engineering named after O.O. Galkin of NAS of
Ukraine, 46 Pr. Nauky, Kyiv 03028, Ukraine

The effect of Cu doping and calcination temperatures on photoluminescence (PL) spectra and XRD patterns of Y-stabilized ZrO_2 powders was studied. The PL spectra of (Y,Cu) codoped samples showed the presence of two main PL components peaked at about 630 and 540 nm in the most samples. The increase of calcination temperature results in the non-monotonic variation of total PL intensity as well as the somewhat changes in PL spectra. The temperature increase from 500°C to 600°C results in the increase of total PL intensity and can be ascribed to the increase of crystallinity degree. The next PL intensity decrease with temperature rise up to 800-900°C is attributed to the appearance of non-radiative recombination centers, probably Zr^{3+}. Their number decrease after annealing at 900-1000°C due to phase transformation from tetagonal to monoclinc as well as the appearance of additional green band can be the reason of consequence PL intensity increase.

Introduction

Zirconia (ZrO_2) has attracted considerable attention because of its mechanical, electric, thermal and luminescent properties offering diverse applications such as catalysts, high temperature and corrosion resistant coatings, sensors, radiation detectors, laser techniques, biological labeling, etc [1-5]. Different defect-related emission bands can be observed in visible spectral range from pure and/or Y-stabilized ZrO_2 materials allowed an application of zirconia for white light emitting devices [6-8].

In recent years, along with ZrO_2 and Y-stabilized ZrO_2 materials, their Cu-doped counterparts have attracted considerable attentions because of promising superplasticity, environmental degradation stability, catalitic activity and tribological behavior [9-12]. These properties were found to be depended on Cu localization and Cu-related substances in the composite. Along with structural properties, they we analyzed in details in the respect to Cu or its compounds located on the surface of ZrO_2 grains. However, in spite of the fact that light emission of these materials allowed the information about composite volume to be extracted, photoluminescence (PL) emission of (Cu,Y)-ZrO_2 materials was not examined well. In present work the interrelation of PL properties and structural characteristics of (Cu,Y)- ZrO_2 nanopowders was investigated versus sintering conditions and Cu content by means of Raman scattering and PL methods.

Experiment

ZrO$_2$ nanopowders doped with Y and Cu were synthesized by a co-precipitation technique using Zr, Y and Cu nitrates. The 25% NH$_4$OH water solution was used as precipitant. Sediments were mixed for 1 hour at room temperature at pH=9. After this they were washed with distilled water, filtered and then hydrogel was dried in microwave furnace and calcinated at T$_c$=500-1000°C for 2 h. The Y$_2$O$_3$ content in the samples was fixed at 3 mol%, whereas CuO concentration was 1 or 8 mol%. The powder was pressed in the pellets for structural and optical characterization. The structure of the pellets was studied by XRD method using Dron-3 and ARL X'TRA powder diffractometer with CuK$_\alpha$ wavelength (λ=0.15418 nm) with grazing geometry. PL and PL excitation spectra were measured using setup equipped with two monochromators. PL emission was excited by the light of Xe lamp dispersed by grating monochromator MDR-23 in 200-400 nm spectral range. PL spectra were collected using monochromator IKS-12 and photomultiplier tube sensitive in the 450-900 nm spectral range. All measurements were performed at room temperature.

Results

Structural properties of the samples

Typical ZrO$_2$ powders with monoclinic and tetragonal structures demonstrate several XRD reflections in the range of 2θ =25-55°. For the monoclinic phase the peaks observed at 28.05° (11-1), 31.33° (111), 33.98° (002), 34.25° (020), 35.15° (200), 35.71° (10-2), 49.02° (022), 49.89° (220), 50.31° (12-2) and 53.84° (202) are indexed corresponding to JCPDS 37-1484 (11). For tetragonal phase the peaks at 2θ~30.4^o, 35.5^o, 50.5° correspond to (111), (002) and (220) reflections (JCPDS 80-0784).
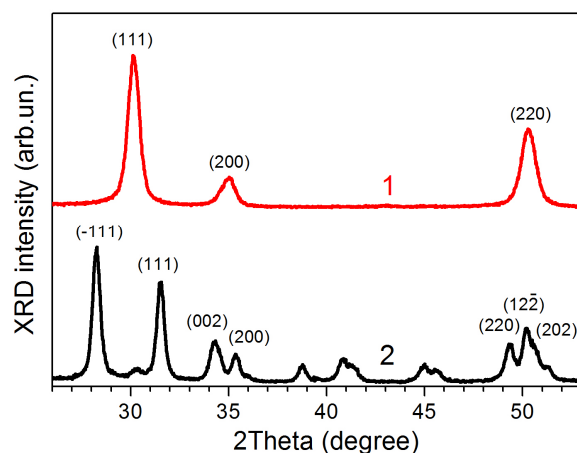
Figure 1. XRD patterns of Y-ZrO$_2$ powders doped with 8 mol % of CuO and calcined at 600°C (1) and 1000°C (2).

As one can see from Fig.1, XRD patterns for the samples with 8 mol% of CuO calcinated at T$_c$=500-800°C represent only tetragonal ZrO$_2$ phase (curve 1). The monoclinic phase (curve 2) appears at T$_c$=900°C and further increase of T$_c$ up at 1000°C results in the increasing of contribution of monoclinic phase up to 55% (Table I). At the same time in the samples with 1 mol% of CuO an appearance of monoclinic phase at low

contribution (~1%) is observed after calcination at T_c=700°C. Higher T_c results in the increases of its contribution increases up to 70% for powders calcined at T_c=1000°C. The crystallite sizes (coherent domain sizes) were estimated from XRD data using Scherrer formula. These results as well as the contribution of tetragonal (T) and monoclinic (M) phases are given in Table I. It is seen that the crystallite sizes gradually increase with T_c rise.

TABLE I. Phase composition and coherent domain sizes in the samples with 1% and 8% of CuO at different calcination temperatures.

Calcination temperature, °C	1 mol% Cu		8 mol% Cu	
	Phase	Coherent domain size, nm	Phase	Coherent domain size, nm
500	100T	11	100T	11
600	100T	12	100T	12
700	1M-99T	17 (T)	100T	18
800	1M-99T	26 (T)	100T	27
900	23M-77T	34 (T)	19M-81T	34 (T)
1000	70M-30T	40 (T), 55 (M)	55M-45T	39 (T), 42 (M)

Light emitting properties of the samples

Photoluminescence spectra of the (Cu,Y)-ZrO_2 samples with different Cu content are present in Fig. 2 (a,b). In the most samples they contain two broad emission bands with maxima at ~540 nm ("green" PL) and ~630 nm ("orange" PL) as well as the long-wavelength tail extended up to 900 nm. The intensity of "green" PL band is slightly higher than that of "orange" one.
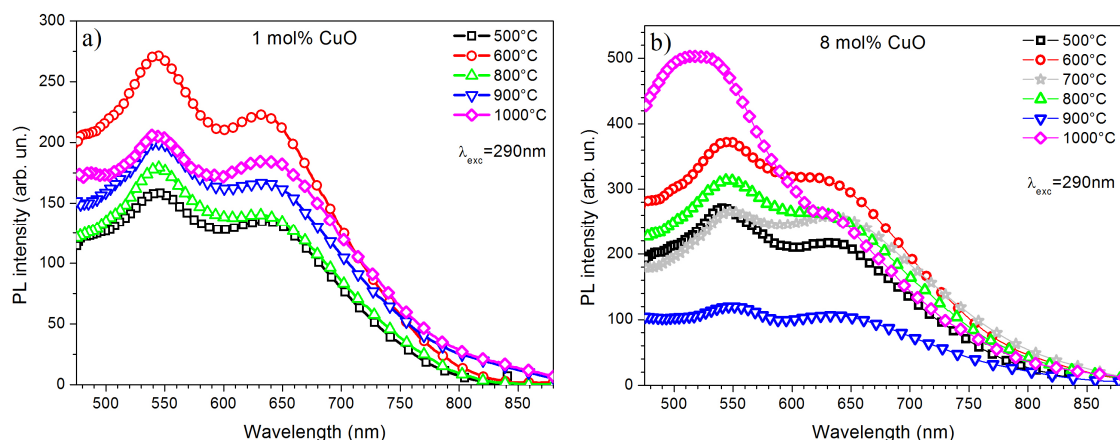
Figure 2. PL spectra of the samples with 1 mol% (a) and 8 mol% (b) of CuO calcined at T_c=500-1000°C. In (a) the PL spectrum for powder calcined at T_c=700°C was not included since it coincided with that for powder calcined at T_c=500°C.

At the same time, in samples with 8 mol% of CuO calcinated at T_c=1000°C the broadening of "green" band and the formation of a plateau near its maximum is observed (Fig.2b, curve 6). This transformation is obviously due to the appearance of additional PL component located near 510 nm. In the samples doped with 1 mol% of CuO and calcined at high T_c, the increase of the PL magnitude in the 450-500 nm spectral range is

apparently caused by the enhancement of the "blue" band usually observed in the Y-ZrO$_2$ materials.

PL excitation spectra were measured for all the samples and were found to be similar for main PL components. The spectra were broad with the maximum near 280 nm (Fig.3).
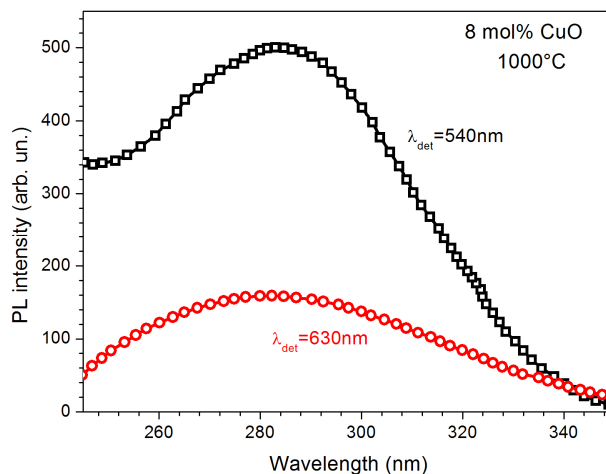
Figure 3. PL excitation spectra of PL band peaked at 540 nm (circle symbols) and 630 nm (square symbols) measured for sample with 8 mol% of CuO.

The intensities of different PL components depend essentially on calcination temperature and Cu content (Fig.4). For the samples doped with 1 mol% of CuO (Fig.4a) besides the dependences for the 540-nm and 630-nm PL components, the corresponding data for the 480-nm one are also shown because of the presence (or appearance) of "blue" PL band in the spectra.
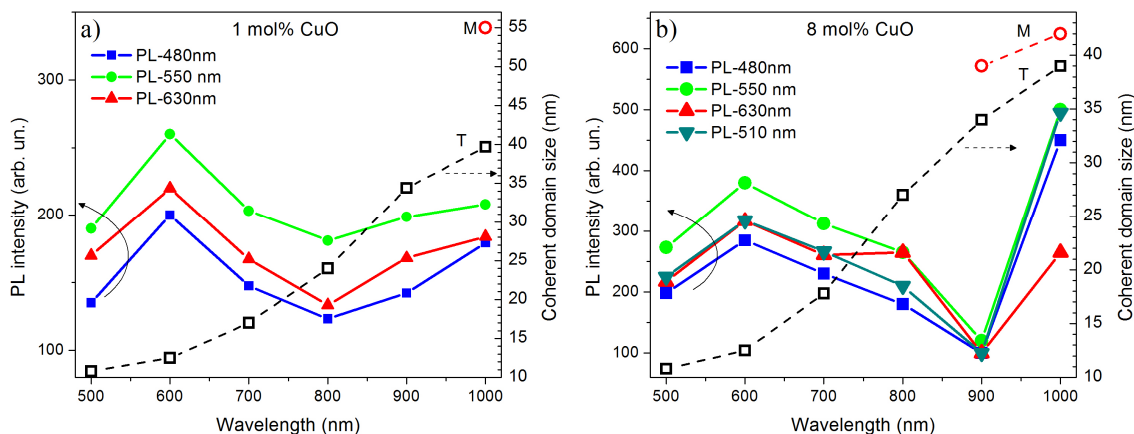
Figure 4. Variation of the intensities of different PL bands and coherent domain sizes on calcination temperature for the powders with 1 mol% of CuO (a) and 8 mol% of CuO (b).

At the same time, for the samples doped with 8 mol% CuO, this evolution is present not only for the 480-nm, 540-nm and 630-nm PL bands, but also for 510-nm one because of an appearance of additional "green" band (Fig.4b). As one can see, the increase of calcination temperature leads to complicated behavior of PL intensity. At first, when T_c increases from 500°C to 600°C, it increases for all the components, then their PL

intensity decreases followed by further rise. The lowest PL intensity for the samples doped with 1 mol% was found for Tc=800°C (Fig.4a).

It is interesting that such variation of PL intensity is more pronounced for the samples with 8 mol% of CuO (Fig.4b). Besides, the increase of CuO content from 1 mol% to 8 mol% results in some difference in the temperature of PL intensity minimum. It is seen from Fig.4b, that the lowest PL intensity for the samples with 8 mol% of CuO became to be observed for higher T_c (900°C). It should be noted that for the samples calcinated at 1000°C the PL intensities of "green" bands increase sharper for the samples with 8% CuO. This is obviously due to an appearance of additional PL band near 510 nm.

The evolution of grain sizes estimated from XRD data on calcination temperature is also shown for the samples with 1 mol% of CuO (Fig.4a) and 8 mol% of CuO (Fig.4b).

Discussion

The results described above show that one of the main features of PL spectra is the non-monotonic variation of PL intensity with calcination temperature. The increase of PL intensity in the temperature range of 500-600°C can be caused by the increase of crystallinity degree. Slower increase of PL intensity, observed for the samples with 8 mol% of CuO in comparison with that for the samples with 1 mol% of CuO, can be connected with the fact that Cu can hamper the crystallization process. Such an effect was earlier observed for Y-ZrO$_2$ powders doped with Cr [13]. The measurements of crystallization temperatures for our samples also confirm this assumption (T=711 K (for Y-ZrO$_2$), 728 K (for (Cu,Y)-ZrO$_2$ with 1mol% of CuO) and 758 K (for (Cu,Y)-ZrO$_2$ with 8 mol% CuO).

Further increase of T_c leads to the decrease of PL intensity for all the bands. Their simultaneous quenching allows concluding that this effect is caused by appearance of fast non-radiative channel of carrier recombination. In common case, this channel can be located at the grains' surface or in their volume. The evolution of grain sizes with T_c shows the decrease of PL intensity when the crystallite sizes increase. The latter means that surface/volume ratio decreases that has to result in the decrease of surface role in recombination processes. Therefore, we can conclude that non-radiative channel is located in the volume of the grains. Because the degree of PL quenching increases with the increase of CuO content we can assume that the appearance of this channel is caused by Cu incorporation in Y-ZrO$_2$ matrix. It is known [14] that this process results in the stabilisation of tetragonal phase leading to formation of oxygen vacancies and Zr^{3+} centers. As it was shown earlier [15,16], the surface Zr^{3+} defect is the center of fast recombination. This allows assuming that Zr^{3+} center in the crystal volume can also serve as non-radiative center which results in the decrease of PL intensity.

The subsequent PL intensity increase correlates with the appearance of monoclinic phase, in which the number of oxygen vacancies (and correspondingly Zr^{3+} centers) decreases. This confirms that the non-radiative channel is connected with the native defects, which number increases with Cu incorporation and decreases with the transformation of tetragonal phase to monoclinic one. The interrelation of nonradiative channel with intrinsic defects confirms also by the coloration of samples investigated. In fact, they have greenish color (Fig.5). Its intensity depends on CuO concentration increasing with its increase. The intensity of this coloration depends also on calcination temperature. With its increase the coloration at first increases and, after appearance of monoclinic phase, it decreases. Because the substances, which can be present on the crystallite surface (CuO, Cu$_2$O, yttrium cuprate), cannot give such a coloration, it can be

assigned to different color centers. It is known that one of the type of color centers are above mentioned intrinsic defects that absorb the light in the range of 300-500 nm [17] and can result in such coloration. Besides, the contribution in sample coloration can give the copper-related center. The increase and decrease of coloration degree correlates with the increase and decrease of the contribution of nonradiative recombination channel.
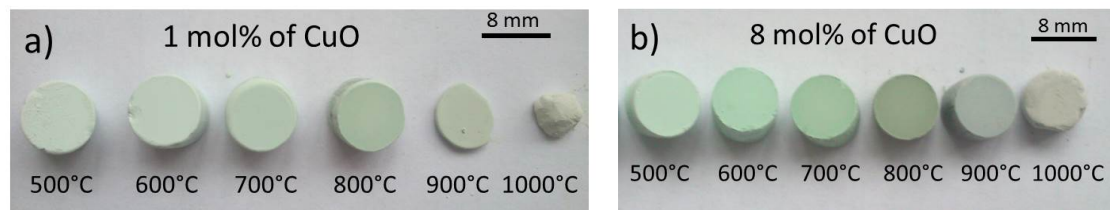
Figure 5. Evolution of the color of pallets of (Cu,Y)-ZrO$_2$ with 1 mol% of CuO (a) and 8 mol% of CuO (b) with calcination temperature.

Thus, the investigation of the dependence of PL intensity on calcination temperature and CuO concentation allows confirming of Cu incorporation into the crystals and concluding that the formation of intrinsic defects or Cu-related centers can result not only in the appearance of radiative centers but also in the enhancement of non-radiative channel. This can be the reason of well-known fact that monoclinic phase has the most bright luminescence.

Besides the PL intensity the somewhat changes in PL spectra was observed that was caused by the appearance or the increase in intensity of additional PL bands. In the samples with 1% of CuO it is blue band while in the samples with 8% of CuO it is new green band at about 510 nm. The blue band is usually observed in ZrO$_2$ with different Y$_2$O$_3$ content while the green band can be caused by defects accompanied the incorporation of Cu atoms in Y-ZrO$_2$ matrix.

Conclusion

The effect of Cu doping on light emitting and structural properties of (Cu,Y)-ZrO$_2$ powders produced by a co-precipitation technique from Zr, Y and/or Cu nitrates was investigated versus copper content and calcination temperature. The samples sintered at T$_c$=500-800°C showed the presence of tetragonal phase predominantly, whereas the further T$_c$ increase results in appearance of significant contribution of m-ZrO$_2$ demonstrating the t-m phase transformation. The higher Cu content in the powders, the higher T$_c$ of t-m phase transition was observed. Along with two main PL components (peaked at 540 and 630 nm) observed for Y-ZrO$_2$ samples, their doping with 8 mol% of CuO stimulates an appearance of additional green PL band (at ~510 nm) in the powders sintered at 1000°C. An annealing at 500-1000 °C results in the non-monotonic variation of total PL intensity as well as the somewhat changes in PL spectra. The increase of calcination temperature from 500°C to 600°C resulted in the increase of total PL intensity can be ascribed to the increase of crystallinity degree. The next its decrease with temperature rise (up to 800-900°C) is caused by the appearance of non-radiative recombination centers, probably Zr^{3+}. The consequent increase of PL intensity can be connected with the decrease of the concentration of these centers due to decrease of oxygen vacancies number under transformation from tetragonal phase to monoclinic one. This correlates with the changes of sample coloration caused by the color centers. The

calcination of the sample with 8 mol% CuO at high temperatures results in the appearance of additional green PL band, which probably connected with the defects caused by Cu incorporation in Y-ZrO$_2$ matrix.

Acknowledgments

References

1. J. D. Fidelus, W. Łojkowski, D. Millers, L. Grigorjeva, K. Smits and R. R. Piticescu, *Sol. St. Phenom.*, **128**, 141 (2007).
2. J. D. Fidelus, W. Lojkowski, D. Millers, K. Smits, and L. Grigorjeva, *IEEE Sensors*, **9**, 1268 (2009).
3. H. Ken Yueh and B. Cox, *J. Nucl. Mat.*, **323**, 57 (2003).
4. R. Jia, W. Yang, Y. Bai, and T. Li, *Opt. Mater.*, **28**, 246 (2004).
5. M. Kim, J. Aarik and I. Sildos, *Nucl. Insrtum. Methods Phys. Res. A*, **537**, 251 (2005)
6. N. G. Petrik, D. P. Tailor and T. M. Orlando, *J. Appl. Phys.*, **85**, 6770 (1999).
7. H. Nakajima and T.Mori, *J. Alloys Compound.*, **408-412**, 728 (2006).
8. K. Smits, L.Grigorjeva, D.Millers, A. Sarakovskis, J. Grabis and W. Lojloeski, *J. Lumin.*, **131**, 2058 (2011).
9. L. Kong, Q. Bi, Sh. Zhu, Zh. Qiao, J. Yang, and W. Liu, *J. Europian Ceram. Soc.*, **34**, 1289 (2014).
10. L. Winnubst, Sh. Ran, E. A. Speets, and D. H. A. Blank, *J. Europian Ceram. Soc.*, **29**, 2549 (2009).
11. Y. Sh. Zhang, L. T. Hu, H. Zhang, J. M. Chen, and W. M. Liu, *J. of Mat. Proc. Technol.*, **198**, 191 (2008).
12. Y. Sun and P.A. Sermon, Catalist Letters, **29**, 361 (1994)
13. T. E. Konstantinova, V. V.Tokii, I. A. Danilenko, G. K. Volkova, S. V. Gorban, N. V. Tokii, and D. L. Savina, *Nanosystems, Nanomaterials, Nanotechnologies*, **6**, 1147 (2008).
14. M. Bhagwat, A. V. Ramaswamy, A. K. Tyagi, V. Ramaswamy, *Mater. Res. Bull.*, **38**, 1713 (2003).
15. N. Korsunska, M. Baran, A. Zhuk, Yu. Polishchuk, T. Stara, V. Kladko, Yu. Bacherikov, Ye. Venger, T. Konstantinova, and L. Khomenkova, *Mater. Research Express*, 1, 045011 (2014).
16. N. Korsunska, V. Papusha, O. Kolomys, V. Strelchuk, A. Kuchuk, V. Kladko, Yu. Bacherikov, T. Konstantinova, and L. Khomenkova, *Phys. Stat. Sol. C*, **11**, 1417 (2014).
17. V. M. Orera, R. I. Merino, Y. Chen, R. Cases, and P. J. Alonso, *Phys. Rev. B*, **42** 9782 (1990).